

## Supporting Information

### **V<sub>2</sub>CT<sub>x</sub> Catalyzes Polysulfide Conversion to Enhance Redox Kinetics of Li–S Batteries**

Fengfeng Han, Qi Jin, Junpeng Xiao, Lili Wu\*, Xitian Zhang\*

*Key Laboratory for Photonic and Electronic Bandgap Materials, Ministry of Education, School of  
Physics and Electronic Engineering, Harbin Normal University, Harbin 150025, people's  
Republic of China.*

---

\* Corresponding author: wll790107@hotmail.com; xtzhazhang@hotmail.com

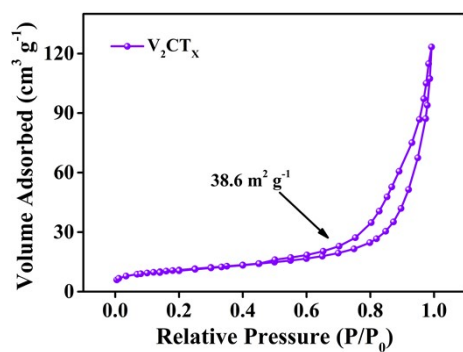


**Fig. S1.** Nitrogen adsorption/desorption isotherm curve of V<sub>2</sub>CT<sub>x</sub> nanobelts.

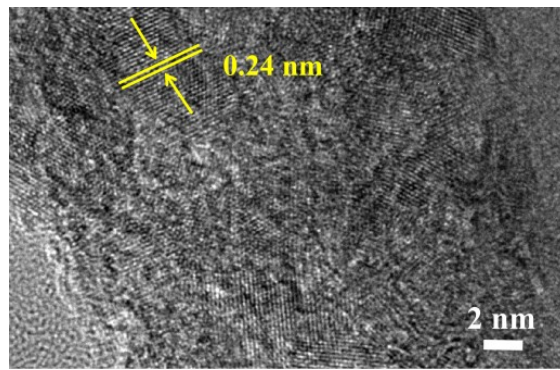


**Fig. S2.** HRTEM image of a V<sub>2</sub>CT<sub>x</sub> nanobelt.

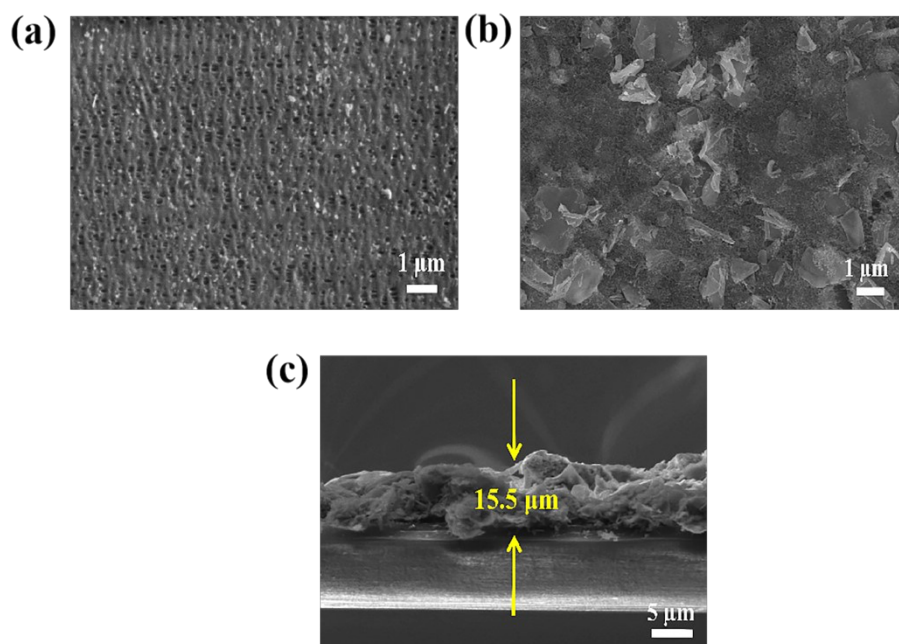


**Fig. S3.** SEM images of (a) PP and (b) KB/V<sub>2</sub>CT<sub>x</sub>-PP separators. (c) Cross-sectional SEM image of KB/V<sub>2</sub>CT<sub>x</sub> interlayer.



**Fig. S4.** Digital photographs of  $\text{Li}_2\text{S}_6$  solution and after the addition of  $\text{KB/V}_2\text{CT}_x$ .

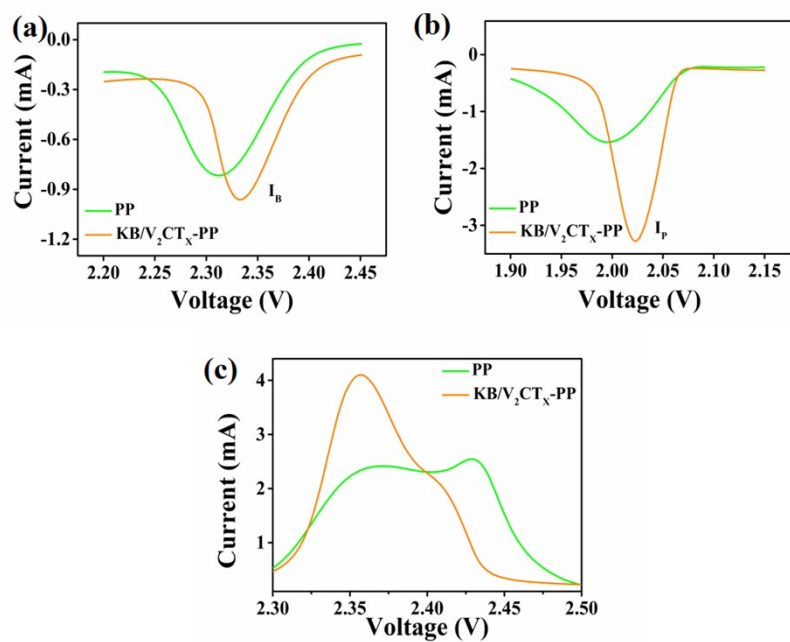


**Fig. S5.** (a, b) Magnified cathodic peaks and (c) anode peaks of the two cells.

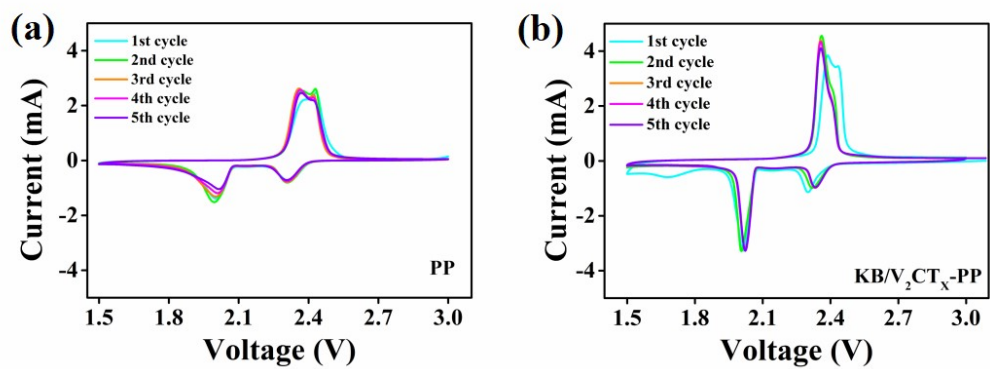


**Fig. S6.** CV profiles of (a) PP and (b) KB/V<sub>2</sub>CT<sub>x</sub>-PP cells for consecutive cycles.

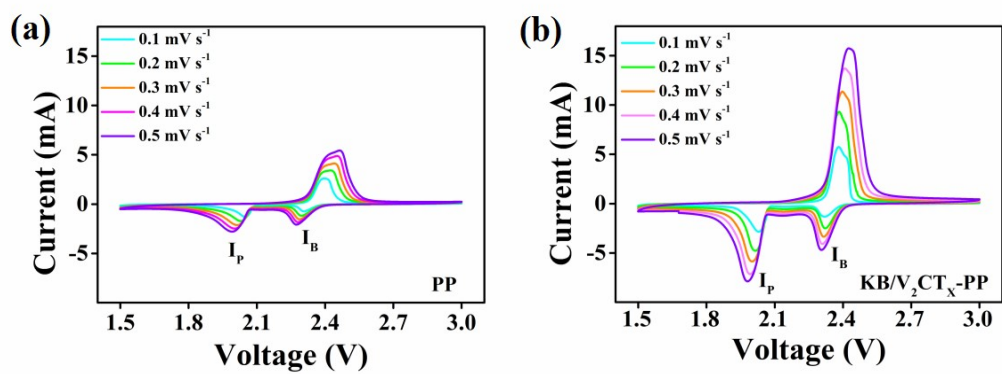
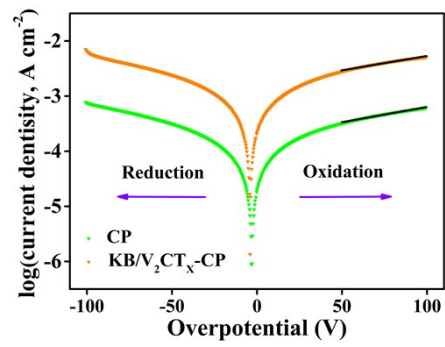
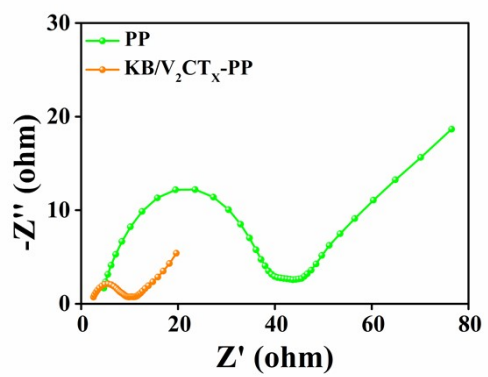


Fig. S7. CV curves of (a) PP and (b)  $\text{KB/V}_2\text{CT}_x\text{-PP}$  cells at different scan rates.





**Fig. S8.** LSV analyses of KB/V<sub>2</sub>CT<sub>x</sub>-CP and CP cells with Li<sub>2</sub>S<sub>6</sub> catholyte.



**Fig. S9.** EIS curves of PP and KB/V<sub>2</sub>CT<sub>x</sub>-PP cells.

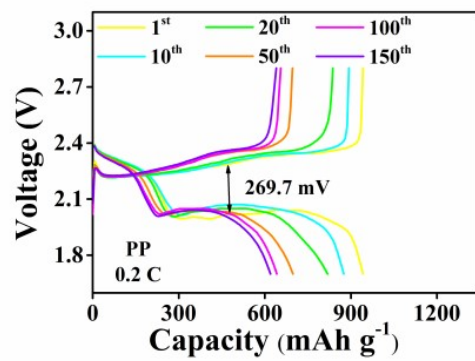


**Fig. S10.** GCD curves of PP cells at 0.2 C.

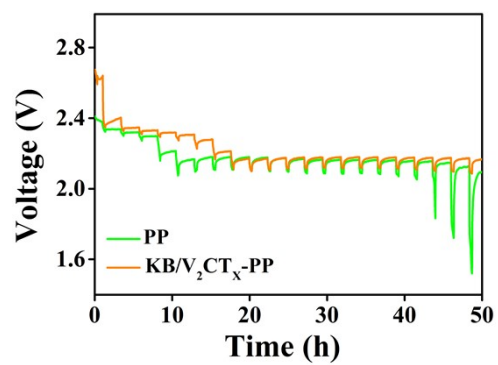


**Fig. S11.** GITT curves of cathodes with PP and KB/V<sub>2</sub>CT<sub>x</sub>-PP separators during discharge process.

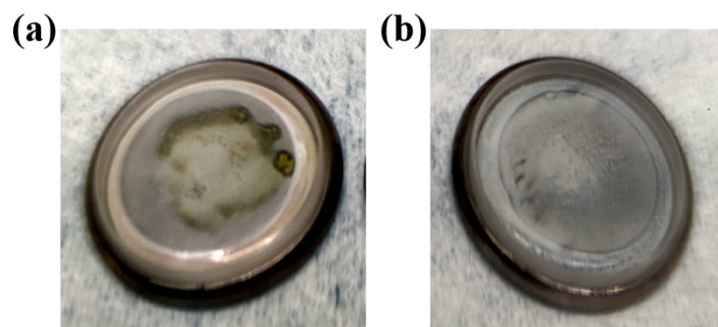


**Fig. S12.** Photographs for (a) PP and (b) KB/V<sub>2</sub>CT<sub>x</sub>-PP separators toward Li metal anode after 150 cycles at 0.2 C.

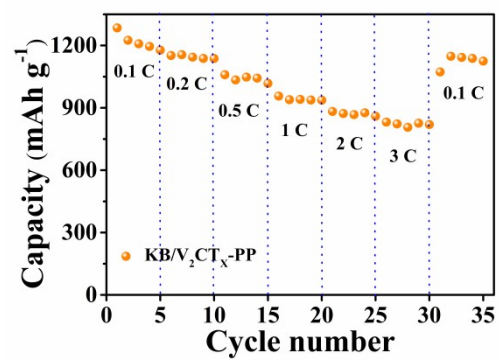


**Fig. S13.** Rate performance of KB/V<sub>2</sub>CT<sub>x</sub>-PP cells (1 C = 1675 mA g<sup>-1</sup>)

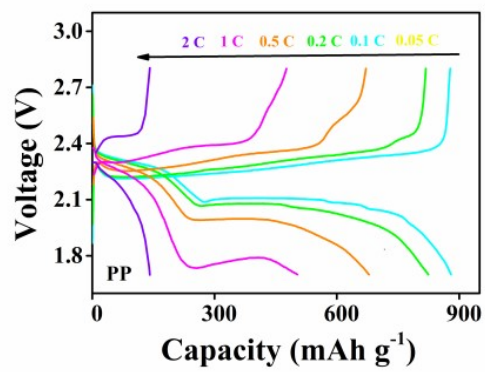


**Fig. S14.** GCD curves of a PP cells at different rates.

**Table S1.** Comparison of the cycle performance between this work and other previously reported similar materials

Materials	S loading (mg cm <sup>-2</sup> )	Rate (C)	Initial capacity (mAh g <sup>-1</sup> )	Cycle Number	Capacity decay (% per cycle)	Ref.
d-Ti <sub>3</sub> C <sub>2</sub>	0.7-1	0.5	899	50	0.64	[1]
Ti <sub>3</sub> C <sub>2</sub> T <sub>x</sub> aerogel	1.2	1	980	1500	0.037	[2]
CNTs/Ti <sub>3</sub> C <sub>2</sub> T <sub>x</sub>	0.8	1	987	600	0.063	[3]
Ti <sub>3</sub> C <sub>2</sub> T <sub>x</sub> @Nafion	2	1	920	1000	0.03	[4]
Nb <sub>2</sub> O <sub>5</sub> -CNT	1.3-1.5	0.2	1286	100	0.23	[5]
S@V <sub>2</sub> C-Li/C	3.0	0.1	1140	100	0.096	[6]
V <sub>2</sub> C/V <sub>2</sub> O <sub>5</sub> /CNTs	2.0	1	1055.2	500	0.034	[7]
KB/V <sub>2</sub> CT <sub>x</sub>	1.2	1	1069	1000	0.049	This work



**Note 1. The detail calculation scheme of relative activation energy.**

CV tests were performed under a scan rate ( $0.1 \text{ mV s}^{-1}$ ) at 298 K as shown in Figure 2a.

Correspondingly, the relationship between electrode potential and activation energy over the Catalyzed-free and In-based batteries could be calculated according to the equation (1):

$$E_a = E_a^0 + \alpha z F \varphi_{cathode}(Ox|Red)_{IR} \quad (1)$$

where  $E_a$  is the activation energy of reduction process,  $E_{a0}$  is the intrinsic activation energy,  $\alpha$  is the symmetry coefficient,  $z$  is the number of charge transfer,  $F$  is the Faraday's constant,  $\varphi_{cathode}(Ox | Red)_{IR}$  is the irreversible potential during cycling.

The Tafel curve calculation formula (2):

$$\eta_{cathode} = \frac{RT}{\alpha z F} \ln j_0 - \frac{RT}{\alpha z F} \ln j_{cathode} \quad (2)$$

where  $\eta_{cathode}$  is the overpotential of the cathode,  $j_0$  is the exchange current density,  $j_{cathode}$  is the current of the cathode. The equation can be written in a more concise form:

$$\eta_{cathode} = a + b \ln j_{cathode} \quad (3)$$

$$b = -\frac{RT}{\alpha z F} \quad (4)$$

where  $a$  is the intercept of Tafel curve,  $b$  is the slop of Tafel curve. Therefore, the equation (1) can be written in a more concise form:

$$E_a = E_a^0 - \frac{RT}{b} \varphi_{cathode}(Ox|Red)_{IR} \quad (5)$$

Based on the intercept and slop of the Tafel curve as shown in Figure. 3b, c the

activation energy during the discharge and charge process can be calculated.

The activation energy corresponding to the reduction of  $S_8$  to the long-chain  $Li_2S_n$ :

$$\text{PP cells: } Ea_1 = Ea_1^0 - 115.77 \text{ kJ mol}^{-1}$$

$$\text{KB/V}_2\text{CT}_X\text{-PP cells: } Ea_1' = Ea_1^0 - 144.4 \text{ kJ mol}^{-1}$$

The difference in activation energy could be calculated by subtracting the activation energy of In-free electrode from that of In-based electrode.

$$Ea_1' - Ea_1 = (Ea_1^0 - 144.4) \text{ kJ mol}^{-1} - (Ea_1^0 - 115.77) \text{ kJ mol}^{-1} = -28.63 \text{ kJ mol}^{-1}$$

The activation energy of long-chain  $Li_2S_n$  to  $Li_2S$ :

$$\text{PP cells: } Ea_2 = Ea_2^0 - 112.32 \text{ kJ mol}^{-1}$$

$$\text{KB/V}_2\text{CT}_X\text{-PP cells: } Ea_2' = Ea_2^0 - 137.14 \text{ kJ mol}^{-1}$$

$$Ea_2' - Ea_2 = (Ea_2^0 - 137.14) \text{ kJ mol}^{-1} - (Ea_2^0 - 112.32) \text{ kJ mol}^{-1} = -24.82 \text{ kJ mol}^{-1}$$

1

## References

- [1] Y.F. Dong, S.H. Zheng, J.Q. Qin, X.J. Zhao, H.D. Shi, X.H. Wang, J. Chen and Z.S. Wu, *ACS Nano*, 2018, 12, 2381-2388.
- [2] Q.H. Meng, Q. Jin, X.Y. Wang, W.B. Lv, X.Z. Ma, L. Li, L.L. Wu, H. Gao, C.C. Zhu and X.T. Zhang, *J. Alloys Compd.*, 2020, 816, 153155.
- [3] N. Li, W.Y. Cao, Y.W. Liu, H.Q. Ye and K. Han, *Colloids Surf. A*, 2019, 573, 128-136.
- [4] J.T. Wang, P.F. Zhai, T.K. Zhao, M.J. Li, Z.H. Yang, H.Q. Zhang and J.J. Huang, *Electrochim. Acta*, 2019, 320, 134558.

- [5] Y.J. Liu, M.Q. Chen, Z. Su, Y.F. Gao, Y.Y. Zhang and D.H. Long, *Carbon*, 2021, 172, 260-271.
- [6] Z. Chen, X.B. Yang, X. Qiao, N. Zhang, C.F. Zhang, Z.L. Ma and H.Q. Wang, J. *Phys. Chem. Lett.*, 2020, 11, 885-890.
- [7] T. Wang, Y.Y. Liu, X.M. Zhang, J.Y. Wang, Y.G. Zhang, Y.B. Li, Y.J. Zhu, G.R. Li and X. Wang, *ACS Appl. Mater. Inter.*, 2021, 13, 56085-56094.
- [8] W.X. Hua, H. Li, C. Pei, J.Y. Xia, Y.F. Sun, C. Zhang, W. Lv, Y. Tao, Y. Jiao, B.S. Zhang, S.Z. Qiao, Y. Wan and Q.H. Yang, *Adv. Mater.*, 2021, 33, 2101006.